Supplement of Clim. Past, 21, 1853–1869, 2025
https://doi.org/10.5194/cp-21-1853-2025-supplement

Supplement of

Quantitative reconstruction of deglacial bottom-water nitrate in marginal Pacific seas using the pore density of denitrifying benthic foraminifera

Anjaly Govindankutty Menon et al.

Correspondence to: Anjaly Govindankutty Menon (anjalygmenon9@gmail.com)

Supplement

Supplement 1

Table S1 The data of calculated ages, mean pore density, reconstructed nitrate of core M77/2-59-01 from Gulf of Guayaquil

Age (ka BP)	Mean Pore density	SD- of pore density	Reconstructed Nitrate	SD_ of Reconstructed Nitrate	SEM
0.188615385	0.004243903	0.00064143	44.46575552	3.074308172	0.50541315
1.152425926	0.004215525	0.000573227	44.57631371	2.857358679	0.469746873
1.363907407	0.003726197	0.000651429	46.48273754	3.023596444	0.497076193
1.469648148	0.004280375	0.000701775	44.32366008	3.274107128	0.538259896
1.78687037	0.00407125	0.000802934	45.13840968	3.579983249	0.588545621
1.998351852	0.004323508	0.000683547	44.15561195	3.22210317	0.529710498
3.1615	0.004097871	0.000597165	45.03469589	2.910316836	0.478453141
3.931681818	0.003798897	0.000524924	46.19949535	2.63634533	0.433412502
4.651375	0.00420308	0.000845447	44.62479942	3.74347414	0.615423358
5.340775	0.003947152	0.000661479	45.62189518	3.090325848	0.50804644
6.05265	0.004160981	0.000623478	44.78881628	3.003550987	0.493780741
6.92185	0.004328553	0.000926989	44.13595761	4.042091673	0.664515778
7.79105	0.004185609	0.000702243	44.69286622	3.260595154	0.536038541
8.429205882	0.003894289	0.000992908	45.82784995	4.221616811	0.694029529
8.928735294	0.004543663	0.000588924	43.29788793	2.965381135	0.487505656
9.428264706	0.004150848	0.000783603	44.82829443	3.525752087	0.579630073
9.927794118	0.003987054	0.000780547	45.46643952	3.492145283	0.574105148
10.42732353	0.004332684	0.000717145	44.11986356	3.332569278	0.547871014
10.92685294	0.004321409	0.000453398	44.16378886	2.531390108	0.41615797
11.4282931	0.004630767	0.00087779	42.95853117	3.914385185	0.64352096
11.93546552	0.004703387	0.000913276	42.67560456	4.046007805	0.665159586
12.44263793	0.004234911	0.000614117	44.5007883	2.98689028	0.491041737

12.94981034	0.003861915	0.000451455	45.95397994	2.433234695	0.40002132
13.30516304	0.003973801	0.000504767	45.5180699	2.608029528	0.428757413
13.56942391	0.004238738	0.000964475	44.48587858	4.161786936	0.684193558
13.83368478	0.004367912	0.000585667	43.98261617	2.922935077	0.480527567
14.09794565	0.004096916	0.000712278	45.0384159	3.279778794	0.539192312
14.36220652	0.004542957	0.000834282	43.30064056	3.754073675	0.617165911
14.62646739	0.005124864	0.000955607	41.0335305	4.251874429	0.69900385
15.03258871	0.004323709	0.001092974	44.15483053	4.628452361	0.760912881
15.45897581	0.00464009	0.001259482	42.92221058	5.264557826	0.865487975
15.8853629	0.005034059	0.001223323	41.38730499	5.178780884	0.851386333
16.31175	0.004421974	0.000883577	43.77198852	3.904559609	0.641905646
16.7381371	0.005259216	0.001044158	40.51009276	4.575720955	0.752243891
17.16452419	0.003767519	0.000485989	46.32174496	2.514716435	0.413416835
17.59091129	0.004026879	0.000742468	45.311279	3.369553157	0.553951127
18.01729839	0.003792185	0.000740117	46.22564662	3.328088637	0.547134402

Table S2 The data of calculated ages, mean pore density, reconstructed nitrate of core MAZ-1E-04 from Mexican Margin

Age (ka BP)	Mean Pore Density	SD-of pore density	Reconstructed Nitrate	SD_of reconstructed nitrate	SEM
2.231537	0.00597494	0.001289	37.72163	5.532069	1.153516
3.715738	0.005733224	0.001002	38.66336	4.502327	0.9388
5.187189	0.005859654	0.000789	38.17079	3.827001	0.797985
8.430525	0.005620055	0.000898	39.10427	4.13475	0.862155
9.393656	0.00554522	0.000897	39.39582	4.121648	0.859423
10.546397	0.005238105	0.001008	40.59234	4.447353	0.927337
11.220128	0.005530394	0.000898	39.45358	4.120619	0.859209
11.766526	0.005909746	0.000878	37.97563	4.122015	0.8595
12.181784	0.004479614	0.000691	43.54742	3.270427	0.681931

12.5091	0.004571004	0.000667	43.19137	3.211799	0.669706
12.896636	0.004632418	0.000885	42.9521	3.940728	0.821699
13.905738	0.004914598	0.000831	41.85272	3.799646	0.792281
14.687318	0.005730131	0.001	38.67541	4.495164	0.937306
15.092991	0.005907214	0.001138	37.98549	4.99279	1.041069
15.580432	0.005922834	0.001064	37.92464	4.740223	0.988405
16.287783	0.00593377	0.000899	37.88203	4.194101	0.874531
16.783407	0.005653819	0.000673	38.97272	3.434485	0.71614
17.376984	0.005598404	0.001035	39.18862	4.593613	0.957835
17.971586	0.005670191	0.000874	38.90893	4.066964	0.848021
18.595875	0.005592348	0.001021	39.21221	4.544021	0.947494
19.12151	0.005274252	0.000653	40.45152	3.299544	0.688002
19.651419	0.005230226	0.000983	40.62304	4.359752	0.909071
20.678308	0.005215462	0.00091	40.68056	4.11276	0.85757

Table S3 The data of calculated ages, mean pore density, reconstructed nitrate of core MD01-2415 from Sea of Okhotsk

Cal. Age (ka BP)	Reconstructed Nitrate	mean pore density	SD of pore density	SD of nitrate	SEM
4.910686	44.08482539	0.004341677	0.000252922	2.068846993	0.623780839
5.835822	41.97988629	0.004881959	0.000464802	2.683066643	0.808975031
6.72318	39.68899396	0.005469971	0.000888046	4.078683963	1.229769486
9.164416	41.49573077	0.005006229	0.000858866	3.907276713	1.178088255
9.382628	42.20871487	0.004823225	0.000812657	3.724787964	1.123065827
9.593771	41.11061769	0.005105078	0.001036783	4.528638785	1.365435969
9.998941799	41.38001081	0.005035932	0.000718335	3.455289311	1.041808926
10.833117	37.47386908	0.006038535	0.000915432	4.264611417	1.285828722
11.894819	38.8260927	0.005691455	0.000883507	4.100785797	1.23643344
12.40353	32.47371424	0.007321942	0.001105856	5.111728351	1.541244088

12.818883	38.82791558	0.005690987	0.000881691	4.094768978	1.2346193

Table S4 The data of calculated ages, mean pore density, reconstructed nitrate of core DSDP-480 from Gulf of California

Cal. Age (ka BP)	Reconstructed nitrate from PD	mean pore density	SD of pore density	SD of nitrate	SEM
10.841384	42.05753576	0.004862029	0.000612252	3.096069	0.774017
11.231995	42.98214584	0.004624706	0.000703065	3.335104	0.833776
11.572385	43.11670541	0.004590168	0.000836496	3.76856	0.94214
14.955692	44.20983142	0.004309592	0.001038735	4.43313	1.108282
17.611215	45.44891754	0.003991551	0.001238435	5.121699	1.280425
18.249825	49.10587561	0.003052907	0.000633977	2.870976	0.717744
18.867347	45.74941911	0.00391442	0.001037673	4.38418	1.096045
19.723566	46.19763339	0.003799375	0.000514765	2.605849	0.651462
19.992225	44.84216069	0.004147289	0.000784469	3.528161	0.88204
20.531769	46.52021192	0.003716578	0.001183442	4.893929	1.223482
21.860501	44.57299537	0.004216377	0.000576201	2.866578	0.716645
22.12605	47.22180129	0.003536499	0.001103217	4.583233	1.145808
22.631367	46.31036985	0.003770439	0.000887086	3.832234	0.958058
23.122318	45.99753219	0.003850736	0.000478896	2.509499	0.627375
25.333737	41.41229463	0.005027645	0.000598406	3.087367	0.771842
25.988473	44.77040267	0.004165708	0.000887401	3.88314	0.970785

Table S5 Bulk sediment nitrogen isotope data of Sea of Okhotsk, Gulf of California, Mexican Margin (from Alcorn et al 2015), and Gulf of Guayaquil (from Mollier-Vogel et al 2019).

Okhotsk_ Age (ka BP)	δ15N_Okhotsk (‰)	California_. Age (ka BP)	δ15N_California (‰)	Mex_. Age (ka BP)	δ15N_Mexico (‰)	Guayaquil_Age (ka BP)	δ15N_Guayaquil (‰)
6.055691	7.562155	0.053323	10.0891257	2.231537	8.688636206	0.188615	3.549191
6.281056	7.1071165	0.502266	10.3529706	3.715738	8.688907568	1.152426	4.208234
6.502271	7.383354	0.841202	10.439908	5.187189	8.766663865	1.363907	4.353331
6.72318	7.5189615	1.146276	10.5541397	8.430525	8.919785057	1.469648	4.428971
6.934847	7.6475375	1.503908	9.8485315	9.393656	8.853831134	1.78687	4.211124
7.168561	7.722875	1.683115	10.8018102	10.546397	8.869239958	1.998352	4.126646
7.41242	7.726893	2.388699	10.5591942	11.220128	8.967896059	3.1615	4.384347
7.677593	7.742965	2.709536	11.3487071	11.766526	8.944345025	3.931682	4.172697
8.013717	8.273341	3.218398	10.6026629	12.181784	9.247560389	4.651375	3.916496
10.022745	9.4094305	3.551827	10.0749731	12.5091	9.13124352	5.340775	4.369743
10.288121	9.44057	3.886275	11.6206392	12.896636	9.134542435	6.05265	4.66364
10.833117	9.171364	4.975366	9.9294035	13.905738	9.401042077	6.92185	4.513473
11.28589	9.4295205	5.317009	10.2549133	14.687318	9.245931846	7.79105	4.506343
11.894819	9.2125485	5.674313	11.3335436	15.092991	8.746991706	8.429206	4.640993
12.709925	8.572682	6.011336	10.0133082	15.580432	7.921292921	8.928735	5.589738
12.818883	8.2582735	6.34564	10.9574888	16.287783	7.653292064	9.428265	5.388674
15.060274	8.389863	6.525673	10.2599678	16.783407	7.43541873	9.927794	5.500757

15.236886	8.281377	6.860886	10.965576	17.376984	7.287496218	10.42732	5.220892
15.448771	8.1437605	7.174359	10.7472216	17.971586	7.230122275	10.92685	5.18536
		7.521942	10.8048429	18.595875	7.398814687	11.42829	5.186013
		7.849065	10.6168155	19.12151	7.581324569	11.93547	5.195337
		8.021876	9.1813375	19.651419	7.338943813	12.44264	5.363324
		8.369174	10.5268454	20.678308	7.06549973	12.94981	5.28939
		8.702521	9.7765112			13.30516	5.831884
		9.785711	11.8844841			13.56942	5.428242
		10.480577	12.4655528			13.83368	5.427035
		10.841384	11.6126098			14.09795	5.8857
		11.231995	11.4410118			14.36221	5.382386
		11.572385	11.6116004			14.62647	5.183455
		12.390675	12.977267			15.03259	5.032097
		12.830288	12.7558799			15.45898	5.094985
		13.262763	12.3828578			15.88536	4.907309
		13.683136	11.875386			16.31175	4.9709
		13.936153	12.6972477			16.73814	4.939713
		14.955692	10.7199273			17.16452	4.351205
		17.030983	10.8058538			17.59091	4.570204
		17.611215	9.0497432			18.0173	4.399932
		18.249825	9.1486644				
		18.867347	9.4474468				
		19.723566	9.117373				
		19.992225	9.2248062				
		20.538763	9.4411388				
		20.954215	6.4364066				

		21.372603	8.4087742				
		21.860501	8.4501596				
		22.12605	8.8862204				
		22.631367	8.8366206				
		23.122318	9.3354034				
		23.872081	8.2866368				
		24.884516	8.5510996				
		25.321483	8.8842016				
		25.735989	6.8805426				
		26.114859	9.2607078				
		26.138731	8.183678				

Table S6 Data of Total Organic Carbon (TOC), dry bulk density, sedimentation rate and accumulation rate of core DSDP-480 from Gulf of California.

Cal.Age	TOC [%]	Sedimentation Rate	Accumulation rate	Dry bulk density (g/cm3)
0	3.3	95.55964	0.582524291	0.184725
0.201301	3.3	95.55964	0.582524291	0.184725
0.326082	3.4	95.55964	0.600176542	0.184725
0.439699	3.3	95.55964	0.582524291	0.184725
0.54614	3.2	95.55964	0.564872039	0.184725
0.649509	3.4	95.55964	0.600176542	0.184725
0.754399	3.2	95.55964	0.564872039	0.184725
0.856334	3	95.55964	0.529567537	0.184725
0.957049	3.3	95.55964	0.582524291	0.184725
1.057975	3.3	95.55964	0.582524291	0.184725
1.160873	3	95.55964	0.529567537	0.184725
1.258923	3.2	95.55964	0.564872039	0.184725
1.358285	3.4	95.55964	0.600176542	0.184725
1.455482	3.3	95.55964	0.582524291	0.184725
1.560095	3.2	95.55964	0.564872039	0.184725
1.662388	3.3	95.55964	0.582524291	0.184725
1.770182	3.1	95.55964	0.547219788	0.184725
1.878806	3.1	95.55964	0.547219788	0.184725
1.983875	3.4	95.55964	0.662006307	0.203755
2.088719	3.4	95.55964	0.662006307	0.203755
2.195552	3.1	95.55964	0.603593986	0.203755
2.301659	3.1	95.55964	0.603593986	0.203755
2.404068	3.1	95.55964	0.608427214	0.205387
2.50241	3.2	95.55964	0.633043038	0.207018
2.596616	3	95.55964	0.598155166	0.20865

2.691844	3	95.55964	0.602832484	0.210281
2.801058	3.2	95.55964	0.648010455	0.211913
2.898063	3.1	95.55964	0.632593357	0.213545
2.993854	3.2	95.55964	0.657988734	0.215176
3.090307	3.2	95.55964	0.662977873	0.216808
3.197104	3.2	95.55964	0.667967012	0.218439
3.298528	3.5	95.55964	0.736045791	0.220071
3.397169	3.4	95.55964	0.720316871	0.221702
3.497384	3.2	95.55964	0.68293443	0.223334
3.598037	3.1	95.55964	0.666425957	0.224965
3.695937	3.1	95.55964	0.671259186	0.226597
3.796983	3.1	95.55964	0.676092415	0.228229
3.903313	3.3	95.55964	0.72485633	0.22986
5.062872	3.1	95.55964	0.736507772	0.248623
5.268917	3.2	95.55964	0.770244366	0.251886
5.373666	3.4	95.55964	0.823685599	0.253518
5.480171	3.1	95.55964	0.755840687	0.255149
5.584727	2.9	95.55964	0.711598179	0.256781
5.690965	2.7	95.55964	0.666732029	0.258412
5.796496	2.7	95.55964	0.670941615	0.260044
6.502269	3.4	95.55964	0.881996164	0.271465
6.600277	3.1	95.55964	0.809006201	0.273096
6.701387	3.2	95.55964	0.840092315	0.274728
6.800861	3.6	95.55964	0.950716636	0.276359
6.907596	2.9	95.55964	0.770376475	0.277991
7.007628	3.2	95.55964	0.855059732	0.279622
7.109446	3.1	95.55964	0.833172344	0.281254
7.210182	3.3	95.55964	0.892070449	0.282886

7.313649	3.1	95.55964	0.842838802	0.284517
7.411119	3	95.55964	0.820327771	0.286149
7.507875	3.1	95.55964	0.852505259	0.28778
7.60373	3.4	95.55964	0.940306728	0.289412
7.710862	3.1	95.55964	0.862171716	0.291043
7.80408	3	95.55964	0.839037043	0.292675
7.902966	2.9	95.55964	0.815590549	0.294306
8.002138	3.1	95.55964	0.876671402	0.295938
8.104068	3.1	95.55964	0.88150463	0.29757
8.202257	2.9	95.55964	0.829154771	0.299201
8.308992	2.8	95.55964	0.804928724	0.300833
8.416008	3	95.55964	0.867100951	0.302464
8.524314	2.9	95.55964	0.842718994	0.304096
8.622372	3	95.55964	0.876455587	0.305727
8.716442	3.1	95.55964	0.910504002	0.307359
8.814755	3.1	95.55964	0.915337231	0.30899
8.911786	3.3	95.55964	0.979536295	0.310622
9.759203	3	95.55964	0.930244744	0.32449
9.968535	2.9	95.55964	0.899236586	0.32449
10.07282	2.8	95.55964	0.868228428	0.32449
10.17645	2.8	95.55964	0.868228428	0.32449
10.28362	2.7	95.55964	0.83722027	0.32449
10.38783	2.8	95.55964	0.868228428	0.32449
10.49724	2.8	95.55964	0.868228428	0.32449
10.60672	2.7	95.55964	0.83722027	0.32449
10.71594	3	95.55964	0.930244744	0.32449
10.82412	2.7	95.55964	0.83722027	0.32449
10.94006	2.9	95.55964	0.899236586	0.32449

11.05471	2.8	95.55964	0.868228428	0.32449
11.17557	2.7	95.55964	0.83722027	0.32449
11.48816	2.8	95.55964	0.868228428	0.32449
11.86989	2.6	25.64372	0.216349493	0.32449
12.15771	2.7	69.3949	0.607984948	0.32449
12.31397	2.7	69.3949	0.607984948	0.32449
12.45062	2.8	69.3949	0.630502909	0.32449
12.58307	2.4	69.3949	0.540431065	0.32449
12.71886	2.4	69.3949	0.540431065	0.32449
12.84992	2.7	69.3949	0.607984948	0.32449
12.97969	2.4	69.3949	0.540431065	0.32449
13.11367	2.6	69.3949	0.585466987	0.32449
13.24298	2.4	69.3949	0.540431065	0.32449
13.37225	2.4	69.3949	0.540431065	0.32449
13.49995	2.4	69.3949	0.540431065	0.32449
13.62693	2.6	69.3949	0.585466987	0.32449
13.74941	2.3	69.3949	0.517913104	0.32449
13.86694	2.2	69.3949	0.495395143	0.32449
13.9961	2.2	69.3949	0.495395143	0.32449
13.9961	2.3	69.3949	0.517913104	0.32449
14.26578	2.4	69.3949	0.540431065	0.32449
14.40075	2.2	69.3949	0.495395143	0.32449
14.55009	2.5	69.3949	0.562949026	0.32449
14.75955	2.6	69.3949	0.585466987	0.32449
15.24604	2.9	64.6024	0.607922424	0.32449
15.38827	2.9	64.6024	1.010426314	0.539334
15.73895	2.6	49.08676	0.6883284	0.539334
15.97964	2.6	49.08676	0.6883284	0.539334

17.33241	2.5	49.08676	0.661854231	0.539334
17.69297	2.5	49.08676	0.661854231	0.539334
18.05357	2.7	49.08676	0.714802569	0.539334
18.33655	2.3	49.08676	0.608905892	0.539334
18.6197	2.4	49.08676	0.635380062	0.539334
19.1322	2.5	49.08676	0.661854231	0.539334
19.65131	2.7	63.98251	0.931714871	0.539334
19.96347	2.5	63.98251	0.862698955	0.539334
20.10897	2.5	63.98251	0.862698955	0.539334
20.40667	2.5	63.98251	0.862698955	0.539334
20.54593	2.5	63.98251	0.862698955	0.539334
20.54593	2.6	63.98251	0.897206913	0.539334
20.68459	2.7	63.98251	0.931714871	0.539334
20.83738	2.7	63.98251	0.931714871	0.539334
20.97329	2.9	63.98251	1.000730787	0.539334
21.10776	2.7	63.98251	0.931714871	0.539334
21.25131	2.7	63.98251	0.931714871	0.539334
21.39433	2.8	63.98251	0.966222829	0.539334
21.54193	2.6	63.98251	0.897206913	0.539334
21.68525	2.9	63.98251	1.000730787	0.539334
21.82621	2.7	63.98251	0.931714871	0.539334
21.96353	2.9	63.98251	1.000730787	0.539334
22.0984	3	63.98251	1.105883944	0.576139
22.24012	3	63.98251	1.105883944	0.576139
22.38418	2.9	63.98251	1.069021146	0.576139
22.52482	2.8	63.98251	1.032158348	0.576139
22.66666	2.8	63.98251	1.032158348	0.576139
22.81171	2.9	63.98251	1.069021146	0.576139

22.96105	3	63.98251	1.105883944	0.576139
23.36164	2.9	63.98251	1.069021146	0.576139

Table S7 Data of Total Organic Carbon (TOC), dry bulk density, sedimentation rate and accumulation rate of core M77/2-59-01 from Gulf of Guayaquil.

Cal. Age (ka BP)	TOC %	Dry bulk density [g/cm³]	Sed. Rate (cm/kyr)	Accumulation rates Corg [g/cm²/ka]
0.035243	3.193			
0.152285	3.083			
0.58848	2.932			
0.870352	2.906			
1.134478	3.25	0.544847	49.06907	0.868891
1.399608	3.118			0
1.669239	3.121	0.544847	49.06907	0.834403
1.924075	2.995	0.555397	49.06907	0.816221
2.191342	2.995	0.576055	49.06907	0.846581
2.483475	2.793	0.58	49.06907	0.794889
2.903509	3.17	0.55	49.06907	0.855519
3.275565	3.125	0.588625	51.86042	0.953949
3.500625	2.924	0.59	51.86042	0.894675
3.739049	3.069	0.57	51.86042	0.90721
4.150212	2.978	0.59	57.79806	1.015523
4.42035	2.895	0.571417	57.79806	0.956125
4.709994	2.971			0
4.850602	2.976			0
5.064004	2.957	0.69	57.79806	1.179271
5.288512	2.962	0.442661	57.79806	0.757825
5.547386	2.849	0.44	57.79806	0.724533
6.042492	2.907	0.67	46.84565	0.912408

6.35459	2.842	0.64	46.84565	0.852066
6.621801	2.86	0.611568	46.84565	0.81937
6.882507	2.769	0.61	46.84565	0.791265
7.141856	2.831			0
7.425516	2.921	0.62	46.84565	0.848384
7.82888	2.735			0
8.162391	2.735	0.63	75.44772	1.300002
8.366228	2.775			0
8.55369	2.8	0.61	75.44772	1.288647
8.728794	2.728	0.722946	75.44772	1.487977
8.902246	2.745	0.72	75.44772	1.491149
9.074014	2.592			0
9.253277	2.579	0.66	75.44772	1.284226
9.432011	2.64	0.640586	75.44772	1.275932
9.603323	2.552	0.64	75.44772	1.232272
9.783323	2.361			0
9.956212	2.39	0.65	75.44772	1.17208
10.142056	2.324	0.673499	75.44772	1.180917
10.32087	2.341	0.673499	75.44772	1.189556
10.503614	2.273			0
10.687585	2.198	0.685435	75.44772	1.136685
10.895827	2.195	0.665819	75.44772	1.102647
11.208704	2.199	0.709666	75.44772	1.177404
11.493066	2.169	0.613961	83.87495	1.116946
11.654819	2.149			0
11.809075	2.132	0.648208	83.87495	1.159135
11.960789	2.083	0.660173	83.87495	1.153398
12.112584	2.073			0

12.269177	2.018	0.666493	83.87495	1.128104
12.423932	1.931	0.628815	83.87495	1.018444
12.572773	1.893	0.683726	83.87495	1.085588
12.751703	1.82			0
13.028026	1.737	0.732671	134.9898	1.717948
13.161686	1.761	0.65761	134.9898	1.563252
13.273946	1.748	0.669763	134.9898	1.580388
13.383997	1.769			0
13.480504	1.716	0.675742	134.9898	1.565306
13.579149	1.712	0.685715	134.9898	1.584706
13.676604	1.723	0.662133	134.9898	1.540038
13.773306	1.752			0
13.872788	1.705	0.63827	134.9898	1.469026
13.971138	1.66	0.628127	134.9898	1.407526
14.066675	1.722	0.667482	134.9898	1.551579
14.165833	1.675			0
14.264897	1.679	0.657702	134.9898	1.490667
14.370793	1.745	0.693126	134.9898	1.632708
14.4807	1.676	0.66401		0
14.6413	1.599			0
14.870704	1.686	0.648345	110.9591	1.212904
15.016982	1.914	0.652804	110.9591	1.386397
15.148116	1.664	0.699929	110.9591	1.29232
15.271892	1.874			0
15.398143	1.948			0
15.521123	1.921			0
15.639744	1.905			0
15.756139	1.765			0

15.873171	1.911	0.691024	110.9591	1.465267
15.991326	1.713	0.690051	110.9591	1.311601
16.113626	1.707	0.688349	110.9591	1.303781
16.236402	1.876			0
16.362816	1.574	0.69	110.9591	1.205082
16.490801	1.743	0.676046	110.9591	1.307485
16.621151	1.571	0.69	110.9591	1.202785
16.743962	1.778			0
16.869356	1.676	0.667795	110.9591	1.24188
16.999944	1.508	0.667475	110.9591	1.116861
17.133371	1.67	0.667795	110.9591	1.237435

Table S8 The data of Total Organic Carbon (TOC), dry bulk density, sedimentation rate and accumulation rate of core MD01-2415 from Sea of Okhotsk.

Cal. Age (kyr BP)	TOC (wt. %)	Sedimentation rate	Dry Bulk Density, g cm-3	TOC AR, g cm-2 kyr-1
0.044105	1.25	34.8	0.86	0.37
0.376611	1.19	34.8	0.88	0.36
0.641229	1.14	34.8	0.89	0.35
0.898056	1.17	34.8	0.72	0.29
1.152006	1.08	34.8	0.84	0.32
1.40654	1.11	34.8	1.07	0.42
1.667762	1.06	34.8	0.87	0.32
1.94059	1.16	34.8	0.86	0.35
2.586348	1.07	20.2	0.89	0.19
3.137628	1.03	20.2	0.83	0.17
3.585649	1	20.2	0.86	0.17
4.017994	0.99	20.2	0.73	0.15
4.457524	1.02	20.2	0.82	0.17

4.910686	1.02	20.2	0.84	0.17
5.367057	0.96	20.2	0.84	0.16
5.835822	0.95	20.2	0.83	0.16
6.281056	0.93	20.2	0.83	0.16
6.72318	0.95	20.2	0.82	0.16
7.168561	0.88	20.2	0.87	0.15
7.677593	0.85	20.2	0.86	0.15
8.492654	0.78	19.8	0.85	0.13
8.950176	0.81	19.8	0.83	0.13
9.382628	0.65	19.8	0.78	0.1
9.512149	0.77	19.8	0.78	0.12
9.713986	1.02	19.8	0.81	0.16
9.796058	1.05	19.8	0.82	0.17
9.928963	1.18	19.8	0.82	0.19
10.171192	0.86	19.8	0.82	0.14
10.288121	1	19.8	0.82	0.16
10.608612	0.83	9.5	0.82	0.06
11.104784	0.67	9.5	0.81	0.05
11.28589	0.76	9.5	0.8	0.06
11.602384	0.68	9.5	0.8	0.05
12.196972	0.61	8.6	0.78	0.04
12.40353	0.54	8.6	0.77	0.04
12.661813	0.74	31.7	0.77	0.18
12.774701	0.82	31.7	0.78	0.2
12.818883	0.83	31.7	0.78	0.2
12.972721	0.56	12.5	0.78	0.05
13.383636	0.43	12.5	0.74	0.04
13.518599	0.36	12.5	0.73	0.03

13.729292	0.4	12.5	0.73	0.04
14.188517	0.56	13.9	0.73	0.06
14.314194	0.45	13.9	0.73	0.05
14.493995	0.41	13.9	0.71	0.04

Table S9 Radiocarbon data used for updating the age-depth model for core MD01-2415 from the Sea of Okhotsk. Based on the data from Bubenshchikova et al 2015.

##	id	ages	ageSds	position	thickness	calCurves	
##1	Top	0	1	0	0	normal	core-top
##2	KIA 45315	2689	25	76	1	marine20	planktic radiocarbon age
##3	Tie1	8200	150	196	1	normal	delta 18O age tie point
##4	KIA 45316	9749	50	242	1	marine20	planktic radiocarbon age
##5	Tie2	11700	150	253	1	normal	delta 18O age tie point
##6	Tie3	12800	150	261	1	normal	delta 18O age tie point
##7	KIA 45317	11504	55	272	1	marine20	planktic radiocarbon age
##8	Tie4	14080	150	286	1	normal	delta 18O age tie point
##9	Tie5	14700	150	295	1	normal	delta 18O age tie point

Table S10. Radiocarbon data used for updating the age-depth model for core DSDP-480 from the Gulf of California. Based on the data from Keigwin & Jones 1990.

depth sed [cm]	Age dated [ka] (Accelerator Mass Spectrometer...)	Age dated std dev [±] (Age, 14C conventional)	Age dated (reservoir correction 301 year...)	Age dated [ka] (reservoir correction 301 year...)
1051	10.8	0.09	10499	10.499
1081	11	0.11	10699	10.699
1101	10.8	0.12	10499	10.499
1111	11	0.13	10699	10.699
1311	13.4	0.11	13099	13.099
1351	13.7	0.21	13399	13.399
1536	17	0.13	16699	16.699
1806	20.6	0.18	20299	20.299

Table S11. Radiocarbon data used for developing the age-depth model for core MAZ-1E-04 from the Mexican Margin.

AWI nr.	sample label	Depth (cm)	age (y)	+-(y)	MRA	MRA corr	Calibrated Age (years BP)
179948	9/1/2022	2.5	260	110	737	0	262.3
184245	MAZ01_E04_37_38P, Mixed planktics	37.5	11,300	90	531	10,769	7,098.5
179943	9/1/2022	39.5	11,800	180	611	11,189	7,456.3
184247	MAZ01_E04_52_53P, T. sacculifer	52.5	9,730	50	522	9,208	10,109.3
9336.1.1	MAZ-1 E-04_58-59 cm, G. ruber	58.5	10,367	101	546	9,821	11,085.3
179944	9/1/2022	59.5	10,600	110	542	10,058	11,354.9
184249	MAZ01_E04_65_66P, T. sacculifer	65.5	10,150	50	634	9,516	11,924.4
9337.1.1	MAZ-1 E-04_78-79 cm, G. ruber	78.5	11,783	109	611	11,172	12,886.7
179945	8/29/2022	79.5	11,350	65	538	10,812	13138.032

184251	MAZ01_E04_85_86P, Mixed planktics	85.5	13,850	85	548	13,302	14831.645
9338.1.1	MAZ-1 E-04_98-99 cm, G. ruber	98.5	13,993	124	620	13,373	15793.264
179946	8/29/2022	99.5	13,550	70	643	12,907	16008.247
9339.1.1	MAZ-1 E-04_119-120 cm, G. ruber	119.5	15,384	136	680	14,704	17883.543
179947	8/29/2022	139.5	17,650	110	877	16,773	20149.511
9340.1.2	MAZ-1 E-04_141-142 cm. G.ruber	141.5	18,064	159	936	17,128	20581.484

Table S12. Radiocarbon data used for updating the age-depth model for core M77/2-59-01 from the Gulf of Guayaquil. Based on the data from Mollier-Vogel et al., 2019.

Depth (cm)	Radiocarbon age (14C yr)	Standard deviation (14C yr)	Ages (Radiocarbon age - Delta R = 200)
13	830	25	630
148	3490	30	3290
203	4325	45	4125
303	5725	50	5525
403	7815	65	7615
658	10470	50	10270
803	11855	60	11655
1033	13140	70	12940
1344	15270	150	15070

Table S13. Site location information of modern [NO_3^-] taken for the nitrate offset from World Ocean Atlas 2018.

Locations	Latitude	Longitude	Water depth (m)	Station ID	[NO_3^-] (μmol/kg)
Gulf of Guayaquil, (M77/2-59-01)	3.5° S	81.5°W	1050	21457 (B)	42.5
Mexican Margin, (MAZ-1E-04)	21.5°N	106.5°W	1450	27910 (B)	42.75
Sea of Okhotsk, (MD01-2415)	53.5°N	149.5°E	850	33729 (B)	43.4
Gulf of California, (DSDP, 480)	27.5°N	111.5°W	750	29197 (B)	35.3

Figures.

Figure S1. Age-depth model updated for core MD01-2415 from the Sea of Okhotsk based on ^{14}C dating and have been calibrated using Marine20. Error bands depict 95% confidence interval.

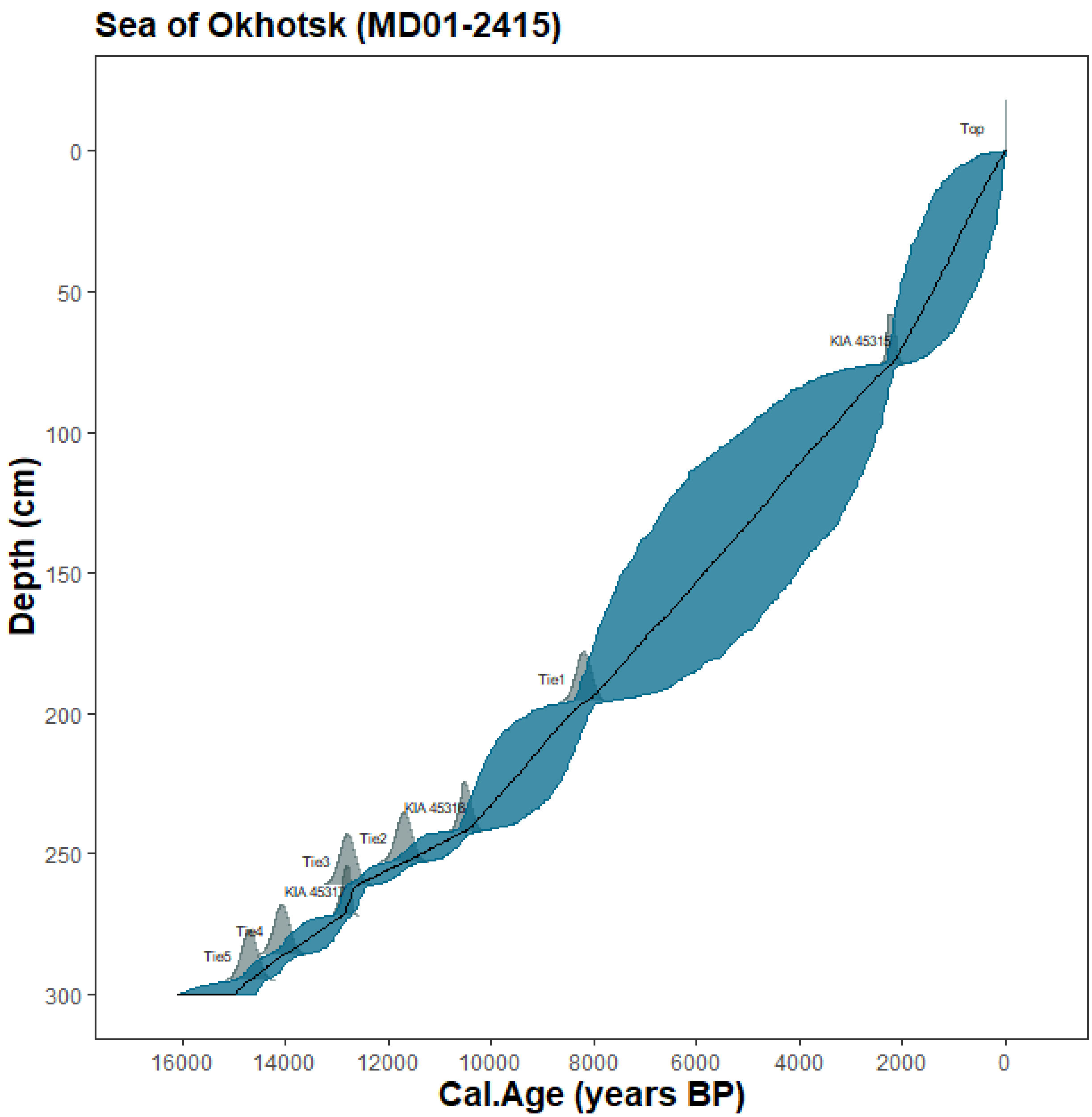

Figure S2. Age-depth model updated for core DSDP-480 from the Gulf of California (Guaymas Basin) based on ^{14}C dating and have been calibrated using Marine20. Error bands depict 95% confidence interval.

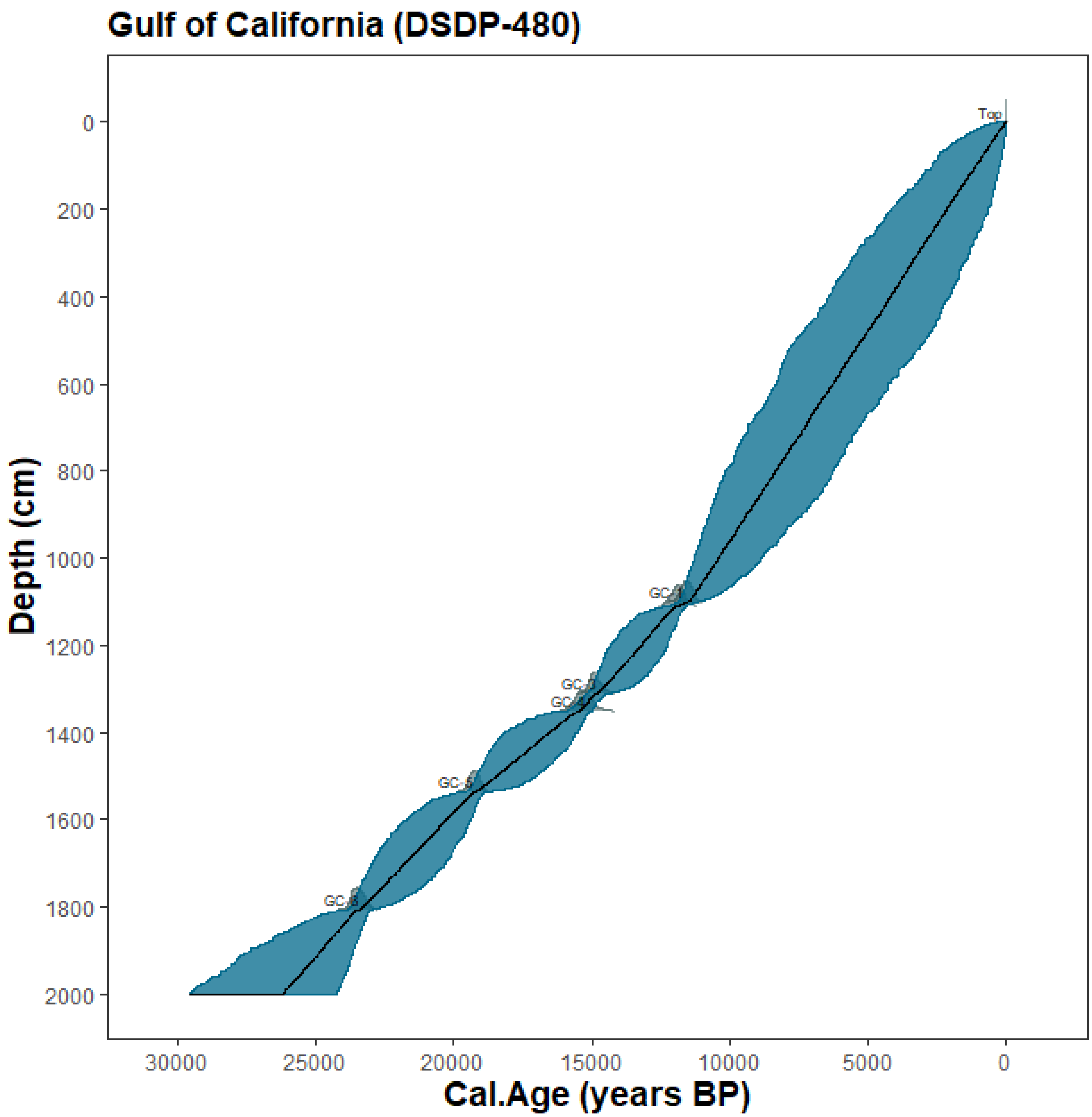

Figure S3. Age-depth model developed in the framework of this study for core MAZ-1E-04 from the Mexican Margin based on ^{14}C dating and have been calibrated using Intcal20. Error bands depict 95% confidence interval. In our radiocarbon data for this core, we had observed age reversals for the top-part above sediment 52.5 cm onwards. This age reversal is shown in the age model. Points "A" and "B" in the figure depicts the age reversal.

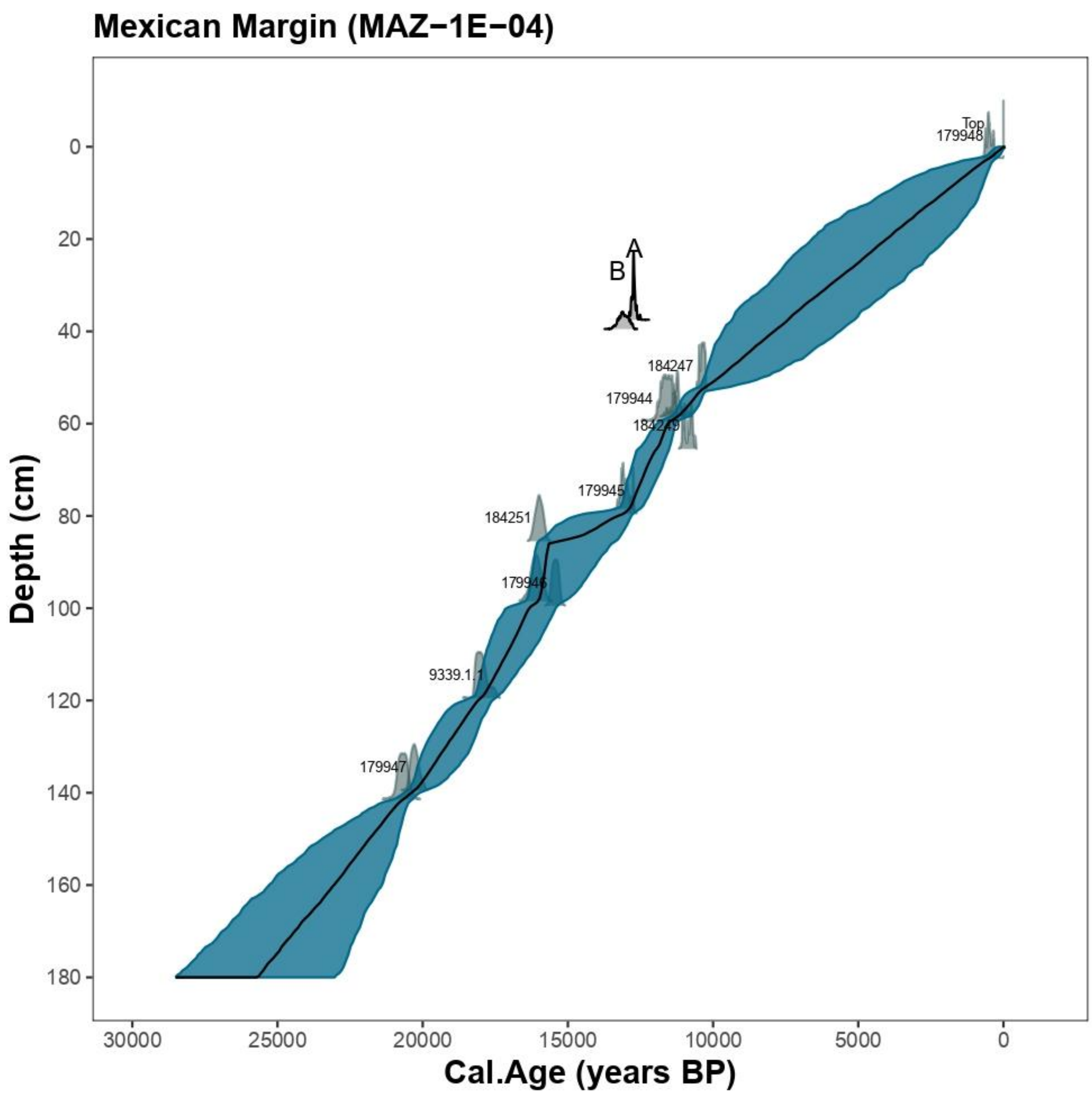

Figure S4. Age-depth model updated for core M77/2-59-01 from the Gulf of Guayaquil based on ^{14}C dating and have been calibrated using Marine20. Error bands depict 95% confidence interval.

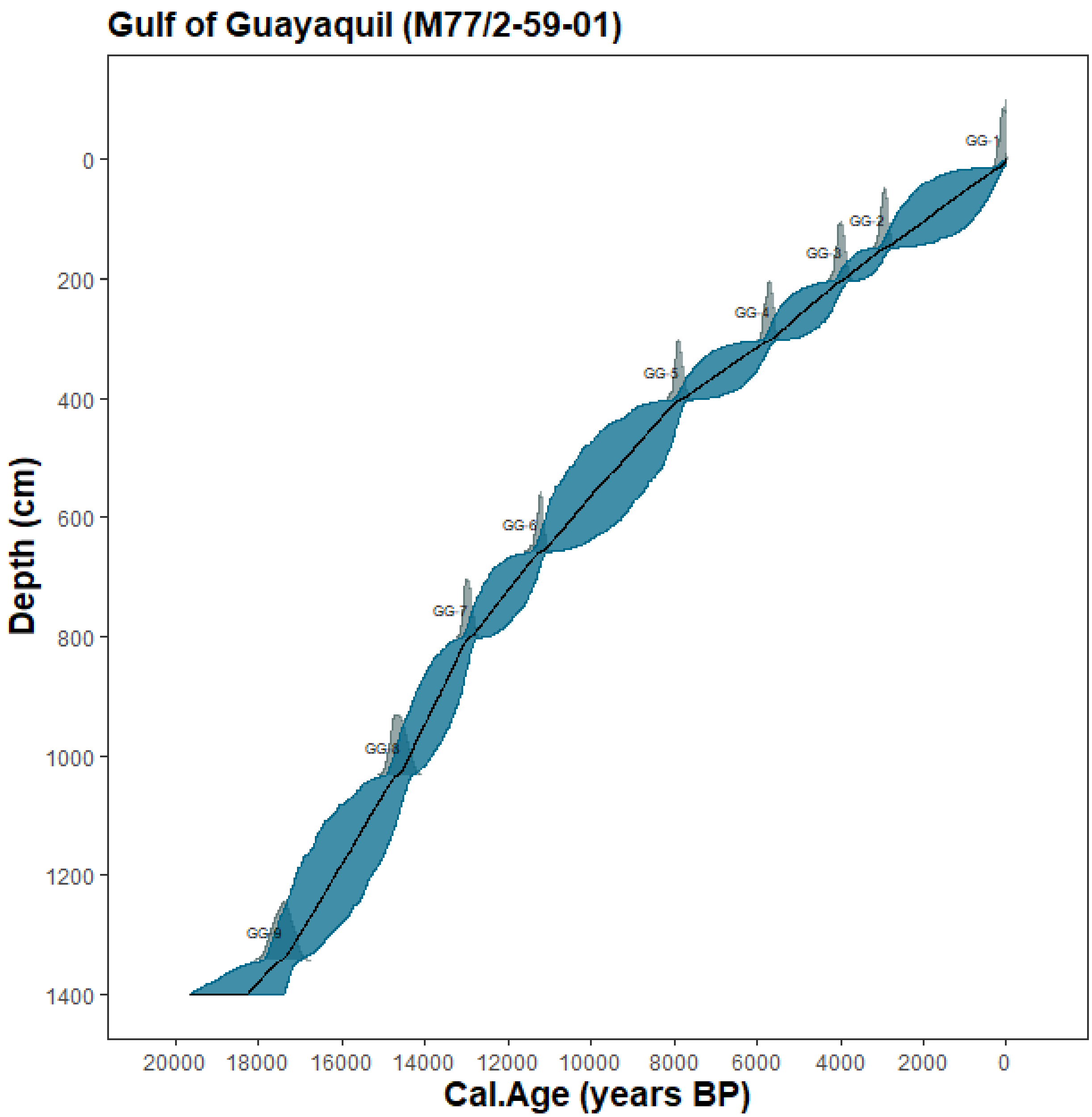

Supplementary Text

Definitions of terms: pore density, porosity and mean pore size

The pore density is the number of pores per unit area, and the porosity is the percentage of the area of the tests occupied by the pores. The mean pore size is the average pore sizes of one individual.

Supplementary Methods

Sampling of foraminiferal specimens for the quantitative nitrate record

A total of 1541 fossil specimens of *B. spissa* (number of specimens, n =1268) and *B. subadvena* (n = 273) were used for the $[NO_3^-]_{BW}$ reconstructions across the four sites. A total of 37 sample depths (n = 669) from the Gulf of Guayaquil (M77/2-059-1), 23 sample depths (n = 455) from the Mexican Margin (MAZ-1E-04), 16 sample depths (n = 273) from the Gulf of California (DSDP-480), and 11 sample depths (n= 144) from the Sea of Okhotsk (MD01-2415) were utilized. Porosity measurements were made on 6-20 well-preserved specimens of *B. spissa* and *B. subadvena* in each sample. The sediment samples were washed and wet-sieved through a 63 µm mesh sieve. The residues were dried in an oven at 38-50°C. The samples were sieved into the grain-size fractions of 63-125, >125-250, >250-315, >315-355, >355-400, and >400 µm. Specimens of *B. spissa*, and *B. subadvena* were picked from the 125-250 µm fraction.

Automated image analysis

For porosity measurements, the total area on the first (oldest) ten chambers (equivalent to an area of 50,000 to 70,000 µm^2) was measured using the ZEN 3.4 blue edition software. The oldest ten chambers are used for the porosity measurements in order to reduce the ontogenetic effect on the pore density and porosity of chambers. The pore parameters such as the pore density (PD), mean pore size, and porosity were determined with the automated image analyzing software Amira™ 3D pro using a previously trained deep-learning algorithm (Govindankutty Menon et al., 2023). The deep learning algorithm was initially trained with manually segmented pores on 52 images of *B. spissa* and 60 images of *B. subadvena*. Only those specimens that had a total area equivalent to at least 50,000 µm^2 were used for the automated analysis. Data from smaller specimens that did not fit within the minimal total area were discarded.

Organic carbon accumulation rates

Organic carbon accumulation rates for cores from the Sea of Okhotsk, the Gulf of California, and the Gulf of Guayaquil were calculated using the sedimentary total organic carbon weight percentage, sediment dry bulk density, and sedimentation rates.

$$\text{TOC Accumulation rate} = \text{Sedimentation rate} \times \text{sediment dry bulk density} \times \text{TOC (wt\%)}$$

The sedimentation rates were calculated from the age-depth model that has been updated within this study. The total organic carbon content and dry bulk densities were taken from Bubenshchikova et al. (2015) for the Sea of Okhotsk, Leclaire and Kerry (1982) for the Gulf of California, and Mollier-Vogel et al. (2019) for the Gulf of Guayaquil. Organic carbon data was not available for core MAZ-1E-04 from the Mexican Margin. High-resolution dry bulk densities were not available for DSDP Site 480 from the Gulf of California. For this core, dry bulk densities have been calculated using the wet dry bulk density and porosity of the sediment shown in figure 24 of Curray et al. (1982). Since the resulting dry bulk data resolution for this core was very sparse for each depth in the core, the dry bulk density of the closest data point was used. There was a large data gap between the 2 m and 9 m sediment depth, with a considerable jump in the dry bulk density between these two sampling depths. Thus, between these two data points, dry bulk densities were linearly interpolated.

Optimization of age models

Marine20 (Heaton et al., 2020) was used to develop the age model for cores from the Sea of Okhotsk, the Gulf of California, and the Gulf of Guayaquil, based on the published ^{14}C ages of planktic foraminifera. However, in Marine20, a continuous reservoir age correction is performed using changes in the globally averaged reservoir age. This is insufficient for local ventilation age reconstructions since reservoir ages vary over time and space. Intcal20 (Reimer et al., 2020) was selected for the Mexican Margin core to maintain consistency with Alcorn et al. (2025, preprint), who also studied this core. Since their work involved detailed benthic ventilation age reconstructions, a more precise manual reservoir age correction was applied.

Sea of Okhotsk: We used the age-tie points and ^{14}C-ages published by Bubenshchikova et al. (2015); based on Nürnberg and Tiedemann, (2004) for the age model of core MD01-2415. The accelerator mass spectrometry (AMS) ^{14}C dates were incorporated in between the age-tie points to minimize the age uncertainty. For the current study, the age-depth model was updated using Marine20 within the Bchron package (Haslett & Parnell, 2008) in RStudio (RStudio Team, 2023) with a local DeltaR of 546 years from the Davydov Cape (Kuzmin et al., 2007).

Gulf of California: We used raw ^{14}C ages of planktic foraminifera from Keigwin and Jones **(**1990) for updating the age-depth model for DSDP Site 480**.** Radiocarbon age calibration was done using Marine20 with a local DeltaR of 301 years from the Guaymas Basin (Goodfriend and Flessa, 1997). The Bchron package was used for determining the age-depth model and calibrating the age.

Mexican Margin: The age model for core MAZ-1E-04 has been entirely built in the framework of the current study. We used planktic foraminifera *Globigerinoides ruber*, *Globigerinoides bulloides*, *Trilobatus sacculifer* for the AMS ^{14}C dating. Approximately 200 tests of these species were selected from the 125-250 µm fraction. The radiocarbon measurements of planktic foraminifera were carried out at the Alfred-

Wegener-Institute (AWI) in Bremerhaven, Germany using the MICADAS system and at the National Ocean Sciences Accelerator Mass Spectrometry Facility, USA. We applied a manual continuous Marine Reservoir Age (MRA) correction using the MRAs from the closest available location to the core MAZ-1E-04 from the published literature (Butzin et al., 2020). Then the corresponding MRAs were subtracted from the raw ^{14}C ages of planktic foraminifers to achieve the atmospheric ^{14}C age. Radiocarbon age calibration was done using Intcal20 in the Bchron package in RStudio.

Gulf of Guayaquil: The published age model of core M77/2-59-01 (Mollier-Vogel et al., 2019) is based on ten AMS ^{14}C ages measured using planktic foraminifera species *Neogloboquadrina dutertrei* at the Leibniz Laboratory at Kiel University, Germany. For the current study, the age-depth model was updated using Marine20 in the Bchron package (Haslett & Parnell, 2008) in RStudio with a DeltaR of 200 ± 50 years (Mollier-Vogel et al., 2013).

Statistical analysis

The statistical analyses presented in this paper were carried out using RStudio, 2023. The t-test was used to test for the significant difference between datasets of unequal sample sizes after carrying out an initial variance test. The confidence interval of 95% ($p < 0.05$) was set for the significance test.

References

1. Curray, J. R., Moore, D. G., Kelts, K., and Einsele, G.: Compilation of detailed examination of Mn deposits from the north tip of the Baja Peninsula prior to DSDP Leg 64 [dataset], PANGAEA, https://doi.org/10.1594/PANGAEA.874590, supplement to: Curray, J. R., Moore, D. G., and others: Tectonics and geological history of the passive continental margin at the tip of Baja California, Initial Reports of the Deep Sea Drilling Project, LXIV, U.S. Government Printing Office, 1089–1136, https://doi.org/10.2973/dsdp.proc.64.150.1982, 1982.

2. Heaton, T. J., Köhler, P., Butzin, M., Bard, E., Reimer, R. W., Austin, W. E., Ramsey, C. B., Grootes, P. M., Hughen, K. A., Kromer, B., Reimer, P. J., Adkins, J., Burke, A., Cook, M. S., Olsen, J., and Skinner, L. C.: Marine20 – the marine radiocarbon age calibration curve (0–55,000 cal BP), Radiocarbon, 62, 779–820, https://doi.org/10.1017/RDC.2020.68, 2020.

3. Butzin, M., Heaton, T. J., Köhler, P., & Lohmann, G.: A short note on marine reservoir age simulations used in IntCal20. Radiocarbon, 62(4), 865-871, https://doi.org/10.1017/RDC.2020.9, 2020.

4. Nürnberg, D. & Tiedemann, R. Environmental change in the Sea of Okhotsk during the last 1.1 million years. Paleoceanography 19, 1–23, https://doi.org/10.1029/2004PA001023, 2004.

5. Haslett J, Parnell AC.: A simple monotone process with application to radiocarbon-dated depth chronologies. J. R. Stat. Soc. Ser. C Appl. Stat., 57, 399–418, https://doi.org/10.1111/j.1467-9876.2007.00613.x, 2008.

6. RStudio Team: RStudio: Integrated Development for R, RStudio, Inc., Boston, MA (2023).

7. Kuzmin, Y. V., Burr, G. S., Gorbunov, S. V., Rakov, V. A., & Razjigaeva, N. G.: A tale of two seas: reservoir age correction values (R, ΔR) for the Sakhalin Island (Sea of Japan and Okhotsk Sea). Nucl. Instrum. Meth. B, 259, 460–462, https://doi.org/10.1016/j.nimb.2007.01.205, 2007.

8. Goodfriend, G. A., & Flessa, K. W.: Radiocarbon reservoir ages in the Gulf of California: roles of upwelling and flow from the Colorado River. Radiocarbon, 39(2), 139-148, https://doi.org/10.1017/S0033822200018175, 1997.

9. Reimer, P. J., Austin, W. E., Bard, E., Bayliss, A., Blackwell, P. G., Ramsey, C. B., Talamo, S., & IntCal Working Group.: The IntCal20 Northern Hemisphere radiocarbon age calibration curve (0–55 cal kBP), Radiocarbon, 62, 725–757, https://doi.org/10.1017/RDC.2020.41, 2020.